Journal of Bioscience and Bioengineering
VOL. 128 No. 1, 22–27, 2019

www.elsevier.com/locate/jbiosc

Establishment of a high throughput-screening system for nucleoside deoxyribosyltransferase II mutant enzymes with altered substrate specificity

Jingmei Li,[1] Lei Yu,[1] Jixuan Li,[1] Liping Xie,[1] Rongqing Zhang,[1,2] and Hongzhong Wang[1,*]

Protein Science Laboratory of the Ministry of Education, School of Life Sciences, Tsinghua University, Beijing 100084, China[1] *and Department of Biotechnology and Biomedicine, Yangtze Delta Region Institute of Tsinghua University, Jiaxing, Zhejiang 314006, China*[2]

Received 17 July 2018; accepted 4 January 2019
Available online 23 February 2019

Nucleoside deoxyribosyltransferase II (NDT) catalyzes the transglycosylation reaction of the 2′-deoxyribose moiety between purine and/or pyrimidine bases and has been widely used in the synthesis of nucleoside analogs. The high specificity of NDT for 2′-deoxyribose limits its applications. Because 2′C- and/or 3′C-modified nucleosides have been widely used as antiviral or antitumour agents, improving the activity of NDT towards these modified nucleosides by protein engineering is an area of interest to the pharmaceutical industry. NDT engineering is hindered by a lack of effective screening methods. This study developed a high-throughput screening system, which was established by nucleoside deoxyribosyltransferase II-cytidine deaminase co-expression, indophenol colorimetric assay and whole-cell catalysis. A high-throughput screening system for NDT was established for the first time. This system can be applied to detect NDT-specific activity for a variety of cytidine analogs with glycosyl and base modifications, such as 5-aza-2′-deoxycytidine, 2′,3′-dideoxycytidine, cytosine-β-D-arabinofuranoside. In this study, we adopted the semi-rational design of NDT and constructed a mutant library of NDT from *Lactobacillus helveticus* (*Lh*NDT) by site-saturation mutagenesis. Over 600 mutants were screened, and a variant with up to a 5.2-fold higher conversion rate of 2′,3′-dideoxyinosine was obtained.

[**Key words:** Nucleoside deoxyribosyltransferase II; High-throughput screening; Substrate specificity; Co-expression; Site-saturation mutagenesis]

Nucleoside deoxyribosyltransferases (NDTs) (EC 2.4.2.6) play a major role in the *Lactobacillus* salvage pathway (1). According to their substrate specificity, NDTs can be divided into type I NDT (PDT), which only catalyzes the transfer of the 2′-deoxyribose moiety between purines, and type II NDT (NDT), which catalyzes the transfer of the 2′-deoxyribose moiety between purine and pyrimidine (2). NDT presents a wide range of base recognition, allowing it to identify a variety of natural and modified bases. Therefore, NDT has been applied to the synthesis of a variety of 2′-deoxynucleoside analogs, such as 5-trifluorothymidine (trifluridine), 5-aza-2′-deoxycytidine (decitabine) (3) and 6-chloropurine-2′-deoxyriboside (4). NDT is highly specific for 2′-deoxynucleoside (5). Many antiviral nucleoside analogs, such as zalcitabine (2′,3′-dideoxycytidine), cytarabine (cytosine-β-D-arabinofuranoside), stavudine (2′,3′-dihydro-2′,3′-deoxythymidine), have deoxyribosyl modifications (6). NDT catalyzes the synthesis of these products with very low efficiency, which limits the application of NDT. Therefore, it is necessary to expand the substrate recognition scope or alter the substrate specificity of NDT by protein engineering.

The NDT structures that have been reported are mainly homohexamers (7–10), tetramers (11,12) and dimers (13,14). Previous studies revealed that NDT monomer is a double-wound α/β domain. NDT active sites are formed by two adjacent subunits (7,8). According to the three-dimensional structure of NDT from *Lactobacillus leichmannii* (*Ll*NDT), deoxyribosyl binding sites are composed of Asp92, Glu98, and Asn123* (* adjacent subunit); base binding sites are composed of Glu46, Asp72 and Tyr157* (* adjacent subunit) (7). These binding sites are conserved in most type II NDTs. Previous studies reported that the transferase reaction follows the Ping-Pong bi bi mechanism (15,16). In the first step, NDT cleaves the C–N bond, releasing the nucleobase. In the second step, the glycosyl intermediate can be attacked by a second nucleobase, leading to a new 2′-deoxyribonucleoside. NDT is highly specific for 2′-deoxynucleoside because Glu98 of NDT forms a hydrogen bond with 3′–OH of 2′-deoxynucleoside. When the sugar donor is a ribonucleoside, Glu98 forms a hydrogen bond with 2′–OH of ribose and the enzyme is inactive (17).

Site-saturation mutagenesis (SSM) is one of the techniques commonly used in the semi-rational design of enzymes. SSM substitutes the amino acid at the particular site to all 20 amino acids based on prior knowledge of the wild-type enzyme (18). SSM has been applied to enhance different catalytic properties, including ligand binding, catalytic activity (19), substrate acceptance (20) and enantioselectivity (21). In this study, we established an SSM library for *Lh*NDT by analyzing the enzyme-substrate interactions and amino acids near the NDT substrate-binding sites. Although the mutant library constructed by SSM has a smaller capacity than the library constructed by random mutagenesis, establishing a high-throughput screening method is still the key step to improving the efficiency of enzyme engineering. Therefore, we developed a

* Corresponding author. Tel.: +86 10 62795632; fax: +86 10 62772899.
E-mail address: hzwang@mail.tsinghua.edu.cn (H. Wang).

1389-1723/$ – see front matter
https://doi.org/10.1016/j.jbiosc.2019.01.002

high-throughput screening system, which involves NDT-cytidine deaminase co-expression and indophenol colorimetric assay. The screening process can be achieved by whole-cell catalysis in 96-well plates.

Cytidine deaminase (CDA, EC 3.5.4.5) catalyzes the irreversible deamination of cytidine to uridine and ammonia (22). CDA has a broad range of substrate acceptance and can catalyze the deamination of a variety of cytidine analogs. The indophenol method has been widely used for ammonia assays in environmental and medical fields (23). Under the catalysis of sodium nitroprusside dehydrate, ammonia reacts with sodium hypochlorite and phenol to form indophenol, which has a maximum absorbance at 630 nm. In this study, uracil-β-D-arabinofuranoside and 2′,3′-dideoxyinosine were used as the sugar moiety donor and cytosine was used as the base acceptor. The catalytic activity of NDT mutants to these nucleoside analogs can be determined by measuring the absorbance of the reaction solution at 630 nm. The scheme of the enzyme-coupled colorimetric assay is shown in Fig. 1.

MATERIALS AND METHODS

Chemicals 2′-Deoxythymidine (dT), 5-aza-2′-deoxycytidine (5-aza-dC), 2′,3′-dideoxyinosine (ddI), 2′,3′-dideoxycytidine (ddC), uracil-β-D-arabinofuranoside (ara-U), cytosine-β-D-arabinofuranoside (ara-C), cytosine (C) and 5-aza-cytosine (5-aza-C) were purchased from Dibo Chemicals (Shanghai, China).

Construction of NDT-CDA co-expression strain The pET-28a(+)-*ndt* and pET-28a(+)-*cda* plasmids were previously constructed in our laboratory. *ndt* gene (GenBank accession number AY064167) and *cda* gene (GenBank accession number X63144) were co-expressed in pET-28a(+) using the ClonExpress II recombinant cloning kit (Vazyme Biotech, Nanjing, China). To ensure the expression of the two genes was comparable, both genes were cloned with an individual T7 promoter. The co-expression plasmid was constructed as reported (24). The primers used in the plasmid construction are listed in Table S1. *Escherichia coli* BL21(DE3) cells (Tiangen Biotech, Beijing, China) were transformed with recombinant plasmid pET-28a(+)-*ndt-cda* and pET-28a(+)-*cda* to form recombinant cell pNC and pC.

These recombinant cells were cultivated in Luria–Bertani medium (LB medium, 1% tryptone, 0.5% yeast extract, 1% NaCl) at 37°C for 12 h. The bacterial suspensions were then inoculated in ZYM-Fe-5052 medium (25) (1% tryptone, 0.5% yeast extract, 25 mM Na_2HPO_4, 25 mM KH_2PO_4, 5 mM Na_2SO_4, 2 mM $MgSO_4$, 100 μM $FeCl_3$, 0.5% glycerol, 0.05% glucose, 0.2% lactose) and cultured at 37°C for 12 h. Both media were supplemented with 100 mg/L kanamycin.

The cell culture was centrifuged (3000 × *g*, 2 min, 4°C) and the cell pellets were suspended with potassium phosphate buffer (50 mM, pH 6.0). The resuspended cells were lysed with sonication (100 × 5 s, interval of 10 s) in ice-water bath. Precipitation and supernatant of recombinant cells were separated by centrifugation (12,000 × *g*, 5 min, 4°C). The expression of NDT and CDA in precipitation and supernatant of recombinant cells was detected by sodium dodecyl sulphate-polyacrylamide gel electrophoretic (SDS-PAGE).

Enzyme activity assay of NDT and CDA Enzyme activity of NDT and CDA from pNC cells was detected with pNC crude enzyme or pNC whole cells. The crude enzyme was prepared as reported previously (26). The NDT activity assay was performed by incubating 1 mg pNC wet cell or pNC 20 μL crude enzyme with 10 mM 2′-dT and 15 mM 5-aza-C in 50 mM, pH 6.0 potassium phosphate buffer. The CDA activity assay was performed by incubating 0.2 mg pNC wet cell or 4 μL pNC crude enzyme with 10 mM 5-aza-dC. The CDA substrate specificity assay used 10 mM dC, ara-C, 5-aza-dC and ddC as the substrate and was performed with CDA crude enzyme. The CDA crude enzyme was prepared with pC cells.

Specific activity of mutant NDT was detected with purified enzyme. Purification of wild-type and mutant NDT was performed as described previously (27). The NDT specific activity assay was performed by incubating 2 μL purified NDT or mutant NDT purified enzyme with 10 mM 2′,3′-dideoxyinosine and 15 mM C in 50 mM, pH 6.0 potassium phosphate buffer.

These reaction mixtures were incubated at 37°C from 5 min to 3 h in volumes of 1 mL and the reactions were then terminated by heating at 100°C for 5 min. The samples were diluted 20-fold with water. The products were detected by high-performance liquid chromatography (Waters 600 HPLC series, Waters Corporation, Milford, MA, USA) with an UV detector at 245 nm. The column was Diamonsil C18 (5 μm, 250 × 4.6 mm) with the column temperature at 25°C. The mobile phase was 15% methanol and 85% water and the flow rate was 1 mL/min.

The protein concentration was detected by the bicinchoninic acid (BCA) protein assay kit (Thermo Fisher Scientific, Shanghai, China) using bovine serum albumin (BSA) as the standard. One unit (U) of NDT or CDA activity was defined as the amount of enzyme required for the synthesis of 1 μmol product within 1 min. The specific activity was defined as the amount of enzyme (mg) producing 1 μmoL/min (U) of product.

Determination of ammonium ion by indophenol colorimetric assay The standard curve of the indophenol assay was generated with NH_4^+ standard solution within a concentration range of 0.156–30 mM. Indophenol colorimetric assay was performed as described previously (28). The proportions of components in the indophenol reaction mixture were adjusted in our study. The reaction mixture contained the following components: NH_4^+ standard solution (0.156–30 mM) or catalytic mixture with pNC cells 10 μL, H_2O 100 μL, reagent A 50 μL (20 mL/L phenol and 1 g/L sodium nitroprusside), and reagent B 50 μL (12.5 g/L sodium hydroxide and 30 mL/L sodium hypochlorite). Reactions were performed at 37°C for 20 min, and reaction mixtures were measured at 630 nm using a microplate reader.

Sensitivity and accuracy of the high-throughput screening system To evaluate the sensitivity of the high-throughput screening system, pNC cells, *E. coli* BL21 cells transformed with an empty pET-28a vector (E28a cells) were cultivated and induced. The culture conditions are described in the mutant screening section. Then, 0.1–3 mg wet cell weight of pNC cells were added to 1 mL standard reaction solution containing 10 mM 2′-dT and 15 mM 5-aza-C in 50 mM, pH 6.0 potassium phosphate buffer. The reactions were performed at 37°C for 1 h in a 96-deep-well plate. Two controls were also performed. One control added E28a cells to the potassium phosphate buffer without substrate (background), and the other added E28a cells to the standard reaction solution (negative control). The concentration of NH_4^+ were detected by the indophenol method. The absorbance was measured by a microplate reader.

To evaluated accuracy of this screening system, the conversion rate of 5-aza-C in the above reaction was determined by high-performance liquid chromatography (HPLC) analysis and compared with conversion rate calculated from the indophenol method. Accuracy of this screening system was further evaluated by incubating 4 μL pNC crude enzyme with 1 mL 5-aza-dC standard solution (0.3–10 mM). After reaction at 37°C for 1 h, the correlation between 5-aza-dC added in reaction mixture and that detected by the enzyme assay was obtained.

Homologous modeling and ligand interaction analysis The protein structure of *Lh*NDT was constructed by an online homology-modeling server SWISS-MODEL (https://swissmodel.expasy.org) by submitting the three-dimensional structure of *Ll*NDT (PDB code 1F8X). Interactions of *Ll*NDT and its ligand (PDB code 1F8Y) were analyzed by Discovery Studio Visualizer 1.6. The amino acids within 6 Å of 2′C and 3′C in the substrate sugar moiety were analyzed. The mutability of amino acids in *Lh*NDT were analyzed by an online sever HotSpot Wizard 2.0 (https://loschmidt.chemi.muni.cz/hotspotwizard/) (29). Mutability scores are predicted by the HotSpot Wizard based on the conservation of amino acid sites and the protein structural information. Sites with high mutability scores

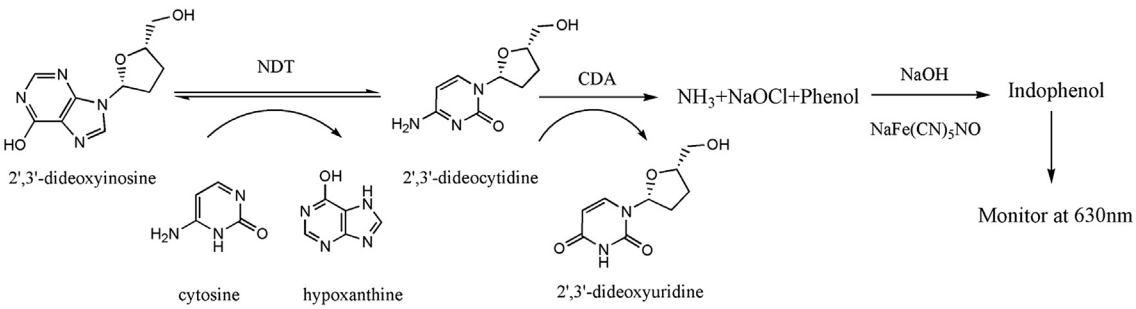

FIG. 1. Principle of nucleoside deoxyribosyltransferase II-cytidine deaminase coupled colorimetric assay. NDT, nucleoside deoxyribosyltransferase (EC 2.4.2.6); CDA, cytidine deaminase (EC 3.5.4.5).

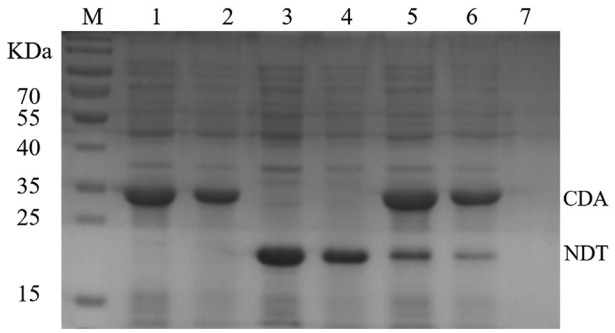

FIG. 2. SDS-PAGE analysis of NDT and CDA. Lane M, molecular weight marker; lanes 1 and 2, sonicated supernatant of recombined pET-*ndt* cells; lanes 3 and 4, sonicated supernatant of recombined pET-*cda* cells; lanes 5 and 6, sonicated supernatant of recombined pNC; lane 7, precipitation of recombined pNC.

are more suitable for mutagenesis. The sites for saturation mutagenesis were selected based on the above analysis results.

Construction of the NDT mutant library The Gly10, Ala11 and Leu96 mutant library was constructed using a QuickChange site-directed mutagenesis kit (Agilent, Beijing, China). pET-28a (+)-*ndt-cda* plasmids were used as a template. The degenerate primers are listed in Table S1. The mutant plasmids were transformed into *E. coli* BL21(DE3) cells, and the mutant strains were grown on an LB agar plate supplemented with 100 mg/L kanamycin.

Mutant screening with recombinant pNC whole cells Mutant NDT screenings with 2′,3′-dideoxynucleoside and arabinofuranoside were performed with pNC whole cells. The *E. coli* BL21 cells transformed with pET-28a vectors were used as the negative control. Randomly picked mutant strains and negative control strains were cultured in 96-deep-well plates containing 500 μL LB medium at 37°C for 12 h. The bacterial suspensions were then inoculated in 96-deep-well plates containing 200 μL ZYM-Fe-5052 medium and cultured at 37°C for 12 h. The induced cells were added to the buffer containing 10 mM ddI and 15 mM C or 10 mM ara-U and 15 mM C (wet cell weight 2 mg/mL). The reactions were performed at 37°C for 1–12 h. The concentration of NH_4^+ was detected by indophenol colorimetric assay and then mutants were screened by a microplate reader. The reaction mixture with high absorbance was screened out and the products in the reaction mixture were further detected by HPLC. Compared with the negative control group, the group with higher conversion rate was selected and the mutant enzyme activity was determined.

RESULTS

Co-expression of NDT and CDA As shown in Fig. 2, CDA exhibited high expression in both pET-*cda* recombinant cells and pNC cells. NDT exhibited high expression in pET-*ndt* recombinant cells but relatively low expression in pNC cells. The absence of protein in the precipitation of pNC cells proved that the decrease of NDT expression was not caused by inclusion body formation. The *cda* gene was cloned from *E. coli* BL21 genomic DNA, but *ndt* is an exogenous gene to *E. coli*; thus, it is possible that the *cda* gene has an expression advantage over the *ndt* gene in *E. coli*.

Enzyme activity assay of NDT and CDA The NDT specific activity of the pNC crude enzyme was 47.8 U/mg, and the CDA specific activity of the pNC crude enzyme was 720.2 U/mg. The NDT specific activity of the pNC whole cell was 0.258 U/mg, and the CDA specific activity of the pNC whole cell was 3.74 U/mg.

The CDA form *E. coli* has been reported to have the deamination activity to the following compounds: 2′-deoxycytidine, 2′-fluoro-2′-deoxycytidine, 5-methyl-2′-deoxycytidine, cytidine, and cytosine-β-D-arabinofuranoside (30). We further determined the deamination activity of CDA to cytosine-β-D-arabinofuranoside and 2′,3′-dideoxycytidine with CDA crude enzyme (Table 1). The pNC cells (1 mg/mL) can completely catalyze the deamination of the 2′-deoxycytidine analogs (10 mM) listed in Table 1 to ammine after reaction for 1 h. Therefore, by measuring the amount of ammonia generated by the NDT-CDA coupled reaction, the conversion rate of NDT can be calculated.

TABLE 1. Substrate specificity of the CDA.

Substrate (10 mM)	Specific activity (U/mg)	Relative activity (%)
2′-Deoxycytidine	1760.8	100
5-Aza-2′-deoxycytidine	816.3	46
Cytosine-β-D-arabinofuranoside	1058.4	60
2′,3′-Dideoxycytidine	72.34	4

Determination of ammonium ion by indophenol colorimetric assay The indophenol colorimetric reaction system was optimized according to the substrate concentration of the NDT standard reaction. When the concentration of NH_4^+ was between 0.156 and 10 mM, the NH_4^+ concentration exhibited high linearity with the absorbance at 630 nm (Fig. 3A).

Sensitivity and accuracy of the high-throughput screening system The catalytic activity of NDT to 2′,3′-dideoxynucleoside and arabinofuranoside is extremely low; thus, these two substrates are not suitable for the construction of colorimetric assays. 5-aza-dC was used as a feature product of NDT to detect the sensitivity and accuracy of the high-throughput screening method.

We compared the absorbance differences among the recombinant strain pNC, and the two controls after the indophenol assay. The absorbance of pNC reaction mixture (2 mg/mL cell concentration) was 20 times higher than that of the background control and negative control (Fig. 3B). Therefore, the screening method exhibits low level of background coloration. The background interference was caused by ammonia produced by *E. coli* fermentation and endogenous deaminase. To ensure accuracy, background control has been done in the following experiment.

To confirm the sensitivity of the screening system, 0.1–3 mg/mL pNC cells were added to the reaction mixture and the conversion rate of 5-aza-C was determined by indophenol method. The conversion rate was calculated from the standard curve of indophenol method. When the concentration of pNC cells was between 0.1 and 3 mg/mL, the background had small interference on the results and the absorbance and conversion rate had good correlations. This system showed high sensitivity with visible color changes at conversion rate from 2.5% to 32.4% (Fig. 3C).

To confirm the accuracy of the screening system, conversion rate of 5-aza-C was also determined by HPLC. When the conversion rate was form 2.5%–32.5%, a good correlation between the colorimetric assay and HPLC was observed (Fig. 3C). The concentration of 5-aza-dC added to the reaction mixture showed high linearity ($R^2 = 0.9998$) with the concentration of 5-aza-dC determined by CDA and the indophenol method (Fig. 3D).

Structure prediction and mutation site selection Sequence alignment showed that the sequence similarity of *Lh*NDT and *Ll*NDT reached 88%. The substrate-binding sites of *Lh*NDT were consistent with the sites reported in *Ll*NDT. The structure of *Ll*NDT and its binding ligand 5-methyl-2′-deoxypseudouridine was analyzed, and the key sites involving enzyme-substrate interactions were obtained (Fig. 4A). Compared with 2′-deoxyribose, arabinose has modifications at 2′C and 2′,3′-deoxyribose has modifications at 3′C. Therefore, we analyzed the amino acids within 6 Å of 2′C and 3′C in 5-methyl-2′-deoxypseudouridine (Fig. 4B). There are fifteen amino acids within 6 Å of 2′C and 3′C, nine of which were conserved sites. Among the remaining six amino acids, Gly9, Ala10 and Leu95 participate in enzyme-substrate interactions. The homologous sites in *Lh*NDT are Gly10, Ala11 and Leu96. Therefore, these three sites were selected to construct the mutant library.

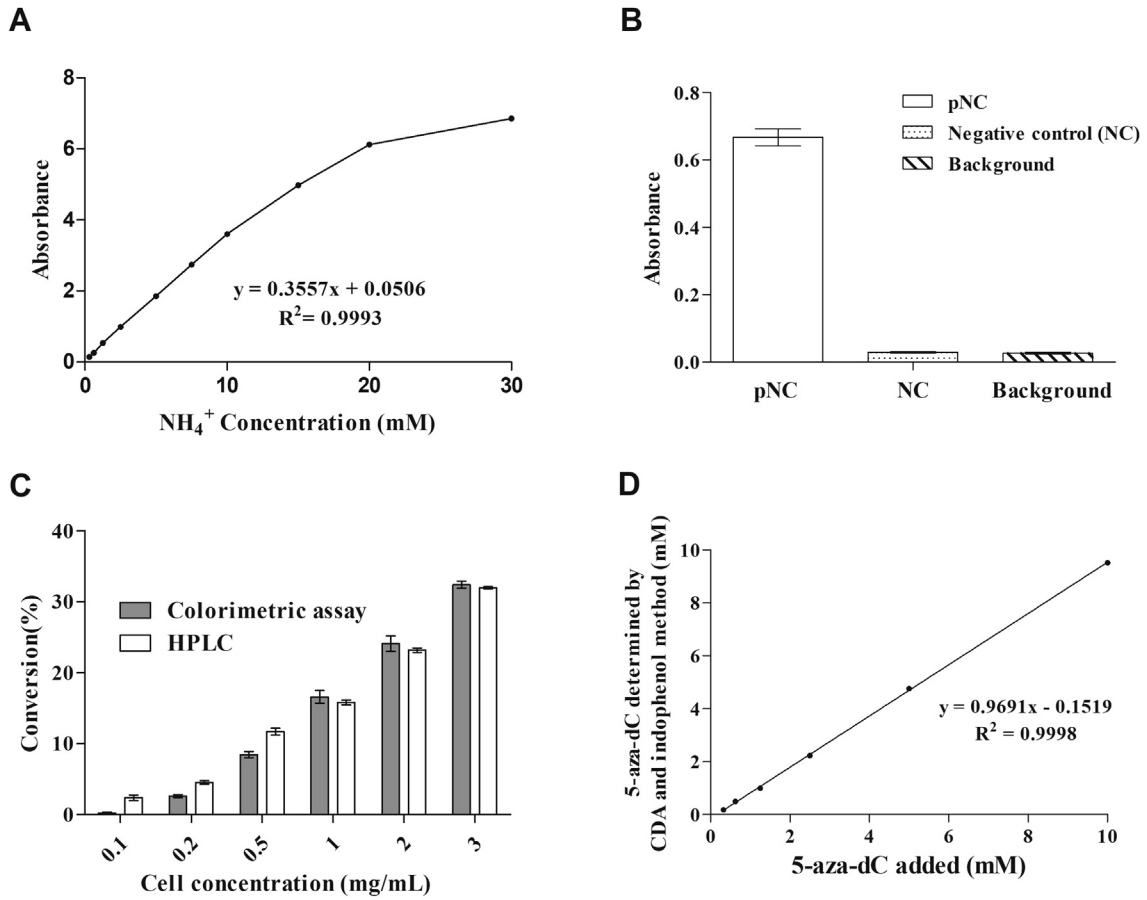

FIG. 3. Construction of the high-throughput screening method. (A) Standard curve of indophenol method. The linear rage is 0.156–10 mM. (B) Background of the high-throughput screening method. Wet cell weight added in reaction mixture is 2 mg/mL pNC: pET-28a(+)-*ndt-cda* recombinant cells; negative control (NC), *E. coli* BL21 cells transformed with pET-28a vector; background: *E. coli* BL21 cells transformed with pET-28a vector, added to pH 6.0 potassium phosphate buffer. (C) Sensitivity of the high-throughput screening method. Wet cell weight of pNC cells added in reaction mixture is 0.1–3 mg/mL. Shaded bars, colorimetric assay; open bars, HPLC assay. (D) Accuracy of the high-throughput screening method. The correlation between concentration of 5-aza-dC added in reaction mixture and that determined by CDA and the indophenol method. (B, C) The standard reaction condition: 10 mM 2′-dT and 15 mM 5-aza-C in 50 mM, pH 6.0 potassium phosphate buffer, performed at 37°C for 1 h. Theses assays were performed in triplicates.

Mutant screening with the recombinant pNC whole cells For 95% library coverage targeting one amino acid, the screening of 96 samples was required in the case of the NNK degenerate codon (31). In this study, approximately 600 mutants were screened with 2′,3′-dideoxynucleoside and arabinofuranoside as substrates. After 12 h of reaction with pNC cells, the concentration of NH_4^+ were detected by the indophenol method. In the 2′,3′-dideoxynucleoside reaction mixture, four mutants with a 4.1-fold increase in absorbance and two mutants with a 1.7-fold increase in absorbance were screened out. DNA sequencing of these mutants showed that the former four mutants were Gly10Ser mutations, and the latter two mutants were Gly10Thr mutations.

Specific activity of wild-type NDT and NDT G10S The enzyme activity of wild-type and mutant NDT was determined with 2′,3′-dideoxyinosine. NDT G10S display improved activity for dideoxynucleoside. The specific activity of NDT G10S is 0.86 U/mg. The specific activity of NDT is 0.13 U/mg. After 12 h of reaction, the conversion rate of 2′,3′-dideoxyinosine catalyzed by NDT G10S can reach 11.9%, which is 5.2-fold higher than that of the wild-type NDT (Fig. S1B and C). As the reaction time increases, ammonia increases in the side reaction, leading to reduced consistency of the conversion rate and absorbance. However, the high-throughput screening system can still accurately screen active mutants.

DISCUSSION

NDT has been reported to have a strict substrate specificity for the 2′-deoxynucleoside. The activity of NDT is generally low towards nucleoside analogs presenting modifications on their 2′-deoxyribose moieties. *Ll*NDT can transfer the sugar moiety from 2′-deoxy-2′-fluorouridine to 1,2,4-triazole-3-carboxamide within 14 days (32). Only NDT from *Lactobacillus reuteri* (*Lr*NDT) has been reported to have relatively moderate catalytic activity for arabinonucleosides, which can catalyze the synthesis of cytosine-β-D-arabinofuranoside within 1 day (9). Thus, genetic engineering is needed to improve the substrate specificity of NDT.

There have been two reports to date on the genetic engineering of NDTs. Kaminski et al. (33) adopted a directed evolution method to obtain NDT mutants with improved 2′,3′-dideoxyribosyltransferase activity. Two mutants, *Ll*NDT G9S and *Lf*NDT A15T, were obtained through random mutagenesis and selection by the uracil auxotrophic strain (33). In their later studies, *Ll*NDT mutants with dNMP, dNDP and dNTP catalytic activity were obtained by rational design and site-directed mutagenesis (34).

In this study, we applied a semi-rational design to *Lh*NDT. The combination of SSM and an enzyme-coupled colorimetric assay is labor-saving, and no detailed protein structure information is required. A variant *Lh*NDT G10S with up to a 6.6-fold higher specific activity for 2′,3′-dideoxyinosine was obtained. *Lh*NDT Gly10 is the homologous site to *Ll*NDT Gly9 identified by Kaminski et al. (33). By

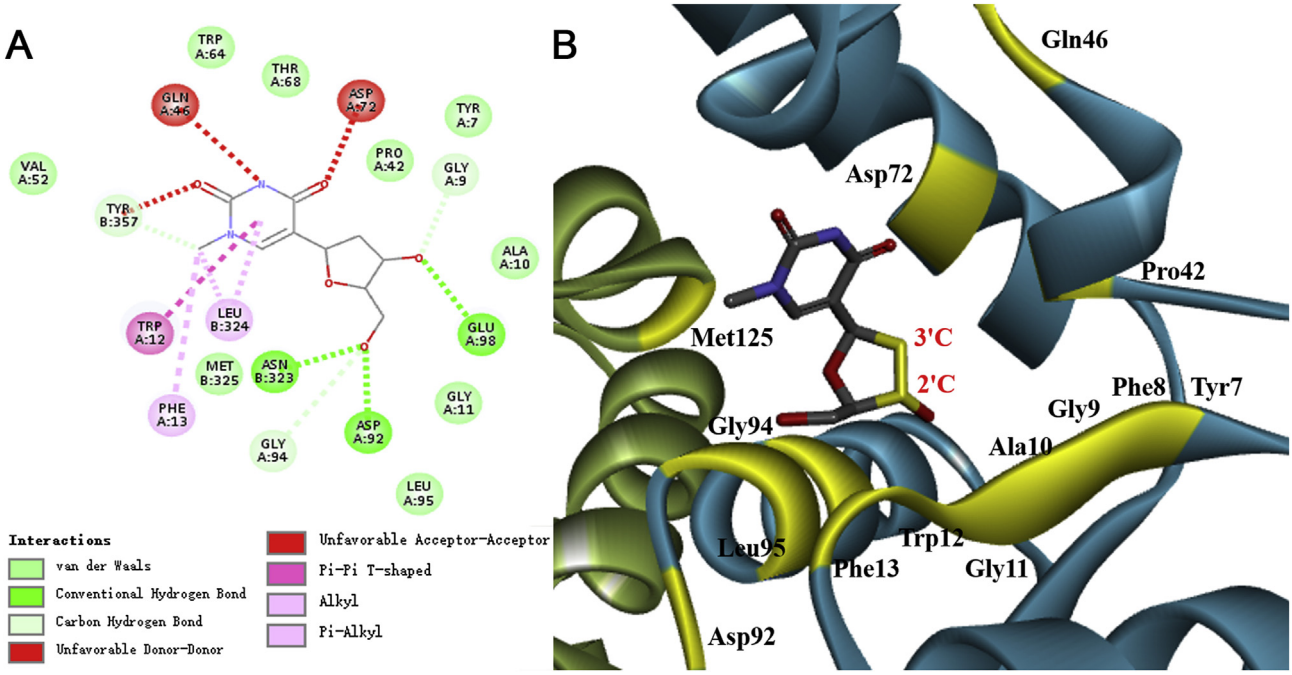

FIG. 4. Model of active sites involved in the enzyme-substrate interaction. (A) Interactions of *Ll*NDT and ligand 5-methyl-2′-deoxypseudouridine on a two-dimensional diagram. (B) The chain A is shown in blue, chain B is shown in green. The amino acids within 6 Å of 2′C and 3′C in substrate sugar moiety are indicated in black. Structure of *Ll*NDT and its ligand (PDB code 1F8Y) were analyzed by Discovery Studio.

SSM, we further confirmed that G10S has the highest activity for 2′,3′-dideoxyinosine among other mutations at Gly10.

The hydrogen bond between 3′—OH of 2′-deoxynucleoside and Glu98 of *Ll*NDT is essential for substrate orientation. The activity of wild-type NDT to the 3′—OH deleted or substituted nucleoside is very low (8). Structure prediction of *Lh*NDT showed that Gly10 is within 6 Å of 3′C in the substrate sugar moiety and Gly10 may interact with 3′—OH of the substrate. Thus, we speculated that the activity for 2′,3′-dideoxynucleosides is improved because the 3′—OH of Ser10 compensates for the missing 3′—OH group in 2′,3′-dideoxynucleosides and interacts with Glu99 of *Lh*NDT. *Lr*NDT is the only NDT among all those reported with relatively strong catalytic activity for arabinonucleosides. Moreover, among the three sites we considered, the homologous sites of Gly10 and Leu96 in *Lr*NDT are Cys12 and Met98. However, we did not obtain mutants with increased arabinonucleoside activity in the mutant library that we constructed. We inferred that similar to ribonucleoside, 2′—OH in arabinose forms a hydrogen bond with *Lh*NDT Glu99. The specificity of NDT for arabinonucleosides may be coordinated by multiple amino acids. The combinatorial site saturation mutagenesis should be applied in subsequent studies.

A high-throughput screening method for the NDT mutant was reported for the first time. The screening method was set up with low background, high sensitivity and high accuracy. As the nucleosides and bases are free to enter and exit cell membranes, the screening procedure was greatly simplified by enzyme co-expression and whole-cell catalysis. The endogenous enzymes such as deaminases and nucleoside phosphorylases in *E. coli* may act on the substrates and products in whole-cell catalysis, thus increasing background in the screening method. A negative control was performed in the screening process showing that the background is relatively low. Selection by an auxotrophic strain used in previous studies is only suitable for NDT with a low initial catalytic activity. Compared with auxotrophic selection, the colorimetric assay used in our study has a broader dynamic range and a better linear relationship. Successful screening of G10S mutants proved the reliability of this screening method. This method can also be applied to screen NDT-specific activity to other modified 2′-deoxynucleosides, such as 2′,3′-didehydro-2′,3′-dideoxynucleosides and 2′-deoxy-2′-fluororibonucleosides, which lays the foundation for the directed evolution of NDT.

Supplementary data to this article can be found online at https://doi.org/10.1016/j.jbiosc.2019.01.002.

ACKNOWLEDGMENTS

This work was supported by the National Natural Science Foundation of China (Grant no. 21476124).

References

1. **Kilstrup, M., Hammer, K., Ruhdal Jensen, P., and Martinussen, J.:** Nucleotide metabolism and its control in lactic acid bacteria, FEMS Microbiol. Rev., **29**, 555—590 (2005).
2. **Becker, J. and Brendel, M.:** Rapid purification and characterization of two distinct *N*-deoxyribosyltransferases of *Lactobacillus leichmannii*, Biol. Chem. Hoppe Seyler, **377**, 357—362 (1996).
3. **Fresco-Taboada, A., Serra, I., Arroyo, M., Fernandez-Lucas, J., Mata, I. D. L., and Terreni, M.:** Development of an immobilized biocatalyst based on *Bacillus psychrosaccharolyticus* NDT for the preparative synthesis of trifluridine and decytabine, Catal. Today, **259**, 197—204 (2016).
4. **Britos, C. N., Lapponi, M. J., Cappa, V. A., Rivero, C. W., and Trelles, J. A.:** Biotransformation of halogenated nucleosides by immobilized *Lactobacillus animalis* 2′-*N*-deoxyribosyltransferase, J. Fluorine Chem., **186**, 91—96 (2016).
5. **Fresco-Taboada, A., de la Mata, I., Arroyo, M., and Fernandez-Lucas, J.:** New insights on nucleoside 2'-deoxyribosyltransferases: a versatile biocatalyst for one-pot one-step synthesis of nucleoside analogs, Appl. Microbiol. Biotechnol., **97**, 3773—3785 (2013).
6. **Seley-Radtke, K. L. and Yates, M. K.:** The evolution of nucleoside analogue antivirals: a review for chemists and non-chemists. Part 1: early structural modifications to the nucleoside scaffold, Antiviral Res., **154**, 66—86 (2018).
7. **Armstrong, S. R., Cook, W. J., Short, S. A., and Ealick, S. E.:** Crystal structures of nucleoside 2'-deoxyribosyltransferase in native and ligand-bound forms reveal architecture of the active site, Structure, **4**, 97—107 (1996).

8. **Anand, R., Kaminski, P. A., and Ealick, S. E.:** Structures of purine 2'-deoxyribosyltransferase, substrate complexes, and the ribosylated enzyme intermediate at 2.0 Å resolution, Biochemistry, **43**, 2384–2393 (2004).
9. **Fernandez-Lucas, J., Acebal, C., Sinisterra, J. V., Arroyo, M., and de la Mata, I.:** *Lactobacillus reuteri* 2'-deoxyribosyltransferase, a novel biocatalyst for tailoring of nucleosides, Appl. Environ. Microbiol., **76**, 1462–1470 (2010).
10. **Fresco-Taboada, A., Fernandez-Lucas, J., Acebal, C., Arroyo, M., Ramon, F., de la Mata, I., and Mancheno, J. M.:** 2'-Deoxyribosyltransferase from *Bacillus psychrosaccharolyticus*: a mesophilic-like biocatalyst for the synthesis of modified nucleosides from a psychrotolerant bacterium, Catalysts, **8**, 8 (2018).
11. **Del Arco, J., Sanchez-Murcia, P. A., Mancheno, J. M., Gago, F., and Fernandez-Lucas, J.:** Characterization of an atypical, thermostable, organic solvent- and acid-tolerant 2'-deoxyribosyltransferase from *Chroococcidiopsis thermalis*, Appl. Microbiol. Biotechnol., **102**, 6947–6957 (2018).
12. **Miyamoto, Y., Masaki, T., and Chohnan, S.:** Characterization of *N*-deoxyribosyltransferase from *Lactococcus lactis* subsp. *lactis*, Biochim. Biophys. Acta, **1774**, 1323–1330 (2007).
13. **Bosch, J., Robien, M. A., Mehlin, C., Boni, E., Riechers, A., Buckner, F. S., Van Voorhis, W. C., Myler, P. J., Worthey, E. A., DeTitta, G., and other 12 authors:** using fragment cocktail crystallography to assist inhibitor design of *Trypanosoma brucei* nucleoside 2-deoxyribosyltransferase, J. Med. Chem., **49**, 5939–5946 (2006).
14. **Crespo, N., Sanchez-Murcia, P. A., Gago, F., Cejudo-Sanches, J., Galmes, M., Fernandez-Lucas, J., and Mancheno, J. M.:** 2'-Deoxyribosyltransferase from *Leishmania mexicana*, an efficient biocatalyst for one-pot, one-step synthesis of nucleosides from poorly soluble purine bases, Appl. Microbiol. Biotechnol., **101**, 7187–7200 (2017).
15. **Danzin, C. and Cardinaud, R.:** Deoxyribosyl transfer catalysis with *trans-N*-deoxyribosylase. Kinetic studies of purine-to-purine *trans-N*-deoxyribosylase, Eur. J. Biochem., **48**, 255–262 (1974).
16. **Danzin, C. and Cardinaud, R.:** Deoxyribosyl transfer catalysis with *trans-N*-deoxyribosylase. Kinetic study of purine(pyrimidine) to pyrimidine(purine) *trans-N*-deoxyribosylase, Eur. J. Biochem., **62**, 365–372 (1976).
17. **Porter, D. J. T. and Short, S. A.:** Nucleoside 2-deoxyribosyltransferase - pre-steady-state kinetic-analysis of native enzyme and mutant enzyme with an alanyl residue replacing Glu-98, J. Biol. Chem., **270**, 15557–15562 (1995).
18. **Porter, J. L., Rusli, R. A., and Ollis, D. L.:** Directed evolution of enzymes for industrial biocatalysis, Chembiochem, **17**, 197–203 (2016).
19. **Choi, Y. H., Kim, J. H., Park, B. S., and Kim, B. G.:** Solubilization and Iterative Saturation Mutagenesis of alpha1,3-fucosyltransferase from *Helicobacter pylori* to enhance its catalytic efficiency, Biotechnol. Bioeng., **113**, 1666–1675 (2016).
20. **Reetz, M. T., Bocola, M., Carballeira, J. D., Zha, D., and Vogel, A.:** Expanding the range of substrate acceptance of enzymes: combinatorial active-site saturation test, Angew. Chem. Int. Ed. Engl., **44**, 4192–4196 (2005).
21. **Li, G., Yao, P., Gong, R., Li, J., Liu, P., Lonsdale, R., Wu, Q., Lin, J., Zhu, D., and Reetz, M. T.:** Simultaneous engineering of an enzyme's entrance tunnel and active site: the case of monoamine oxidase MAO-N, Chem. Sci., **8**, 4093–4099 (2017).
22. **Cohen, R. M. and Wolfenden, R.:** Cytidine deaminase from *Escherichia coli*. Purification, properties and inhibition by the potential transition state analog 3,4,5,6-tetrahydrouridine, J. Biol. Chem., **246**, 7561–7565 (1971).
23. **Searle, P. L.:** The berthelot or indophenol reaction and its use in the analytical-chemistry of nitrogen – a review, Analyst, **109**, 549–568 (1984).
24. **Kim, K. J., Kim, H. E., Lee, K. H., Han, W., Yi, M. J., Jeong, J., and Oh, B. H.:** Two-promoter vector is highly efficient for overproduction of protein complexes, Protein Sci., **13**, 1698–1703 (2004).
25. **Xiong, J., Zhang, W. Q., Su, J. T., Shangguan, J. L., Lin, Y., Yang, Y., Zhang, R. Q., Xie, L. P., and Wang, H. Z.:** Improved synthesis of 2'-deoxyadenosine and 5-methyluridine by *Escherichia coli* using an auto-induction system, World J. Microbiol. Biotechnol., **28**, 721–727 (2012).
26. **Li, Y. Y., Ding, Q. B., Ou, L., Qian, Y. H., and Zhang, J.:** One-pot process of 2'-deoxyguanylic acid catalyzed by a multi-enzyme system, Biotechnol. Bioprocess Eng., **20**, 37–43 (2015).
27. **Lin, Y., Zhang, W., Zhu, F., Su, J., Fang, D., Yang, Y., Zhang, G., Xie, L., Zhang, R., and Wang, H.:** Subcellular localization of *N*-deoxyribosyltransferase in *Lactobacillus fermentum*: cell surface association of an intracellular nucleotide metabolic enzyme, FEMS Microbiol. Lett., **323**, 132–141 (2011).
28. **Dong, H., Liu, Y., Zu, X., Li, N., Li, F., and Zhang, D.:** An enzymatic assay for high-throughput screening of cytidine-producing microbial strains, PLoS One, **10**, e0121612 (2015).
29. **Bendl, J., Stourac, J., Sebestova, E., Vavra, O., Musil, M., Brezovsky, J., and Damborsky, J.:** HotSpot Wizard 2.0: automated design of site-specific mutations and smart libraries in protein engineering, Nucleic Acids Res., **44**, W479–W487 (2016).
30. **Hosono, H. and Kuno, S.:** The purification and properties of cytidine deaminase from *Escherichia coli*, J. Biochem., **74**, 797–803 (1973).
31. **Kille, S., Acevedo-Rocha, C. G., Parra, L. P., Zhang, Z. G., Opperman, D. J., Reetz, M. T., and Acevedo, J. P.:** Reducing codon redundancy and screening effort of combinatorial protein libraries created by saturation mutagenesis, ACS Synth. Biol., **2**, 83–92 (2013).
32. **Slater, M. J., Gowrie, C., Freeman, G. A., and Short, S. A.:** Enzymatic synthesis and antiviral activity of 2'-deoxy-2'-fluoro-ribavirin, Bioorg. Med. Chem. Lett., **6**, 2787–2790 (1996).
33. **Kaminski, P. A., Dacher, P., Dugue, L., and Pochet, S.:** In vivo reshaping the catalytic site of nucleoside 2'-deoxyribosyltransferase for dideoxy- and didehydronucleosides via a single amino acid substitution, J. Biol. Chem., **283**, 20053–20059 (2008).
34. **Kaminski, P. A. and Labesse, G.:** Phosphodeoxyribosyltransferases, designed enzymes for deoxyribonucleotides synthesis, J. Biol. Chem., **288**, 6534–6541 (2013).